



ELSEVIER

Available online at www.sciencedirect.com

SCIENCE @ DIRECT®

Journal of Magnetism and Magnetic Materials 293 (2005) 69–74

Journal of
magnetism
and
magnetic
materials

www.elsevier.com/locate/jmmm

Magnetostructural study of iron sucrose

Lucía Gutiérrez^{a,*}, María del Puerto Morales^b, Francisco José Lázaro^{a,c}

^a*Dept. Ciencia y Tecnología de Materiales y Fluidos, CPS (Univ. de Zaragoza), 50018 Zaragoza, Spain*

^b*Instituto de Ciencia de Materiales de Madrid (CSIC), Cantoblanco, 28049 Madrid, Spain*

^c*Instituto de Ciencia de Materiales de Aragón (Univ. de Zaragoza-CSIC), 50018 Zaragoza, Spain*

Available online 5 March 2005

Abstract

Magnetic and structural analyses have been performed on an iron sucrose complex used as a haematonic agent. The system contains two-line ferrihydrite particles of about 5 nm that are superparamagnetic above approximately 50 K. The observed low-temperature magnetic dynamics of this compound is closer to simple models than in the case of other iron-containing drugs for intravenous use like iron dextran.

© 2005 Published by Elsevier B.V.

Keywords: Iron sucrose; Superparamagnetism; Antiferromagnetic particles; AC susceptibility; Intravenous iron

1. Introduction

Iron sucrose drugs are recently used as an intravenous iron preparation in cases of iron deficiency anaemia, especially for patients undergoing haemodialysis [1]. It is known that other iron-containing drugs, like iron dextran, present in some cases adverse reactions after intravenous administration or are not tolerated as well as iron sucrose [1–5].

In these drugs, iron is commonly present as oxyhydroxide nanoparticles, whose speciation and size play a crucial role because they determine the solubility and diffusion coefficient, eventually

affecting degradation kinetics and biodistribution. Although clinical [3–5] and *in vitro* [6] studies exist on the use of iron sucrose, just few very basic works focus on the physicochemical properties of that compound [7,8].

Previous structural characterisation of nanometric iron oxyhydroxide particles in similar iron-containing drugs, has been performed using Mössbauer spectroscopy, X-ray diffraction and transmission electron microscopy among other techniques [9–12]. For obvious biocompatibility reasons, the iron content in these drugs is low, however, the magnetogenic character of this element makes it possible to obtain interesting and complementary physicochemical data [13,14]. The fact that iron is mostly present as small particles of antiferromagnetic compounds, internally compensating most of the magnetic moment

*Corresponding author. Tel.: +34 976 761958;
fax: +34 976 761957.

E-mail address: lucia@unizar.es (L. Gutiérrez).

content, leads to the necessity of using very sensitive magnetic detection techniques for such characterisation.

In this work, X-ray diffraction, transmission electron microscopy, field- and temperature-dependent magnetisation and dynamic magnetic susceptibility measurements have been performed on iron sucrose. All these techniques have been combined to investigate the sizes and structure of the iron-containing particles, which affect the functionality of the drug. The magnetism of this compound offers another example of the behaviour of antiferromagnetic nanoparticles and, on the other hand, would allow the identification or monitoring, by magnetic means, of this drug in potential studies in the biological medium.

2. Experimental

The iron sucrose sample used in this study was obtained from a commercial pharmaceutical compound called Venofer[®] (VIFOR). The content of one ampoule (5 ml) was freeze-dried during 48 h and the resulting product was used for all the measurements. The iron content of the freeze-dried sample was determined by ICP-AES, in a Perkin Elmer P-40, to be 47.11 mg Fe/g.

Structural analyses were performed by X-ray diffraction and transmission electron microscopy (TEM). The freeze-dried iron-sucrose was milled in a mortar and the powder was used to record the X-ray diffraction patterns between 5° and 90° (2 θ) at 0.5°/min in a Phillips PW1710 diffractometer with Cu K α radiation. TEM analysis was performed in a JEOL 2000 FXII microscope operated at 200 kV. Electron diffraction was carried out on selected areas and the maxima were identified using a thallos chloride diffraction standard to calculate accurately the camera length. The solid was dispersed in acetone in an ultrasonic bath for some minutes. A drop of this liquid was placed on a carbon-coated copper grid and allowed to dry.

The magnetic characterisation was carried out in a Quantum Design MPMS-XL SQUID magnetometer equipped with an AC option. The AC amplitude of the susceptibility measurements was

0.41 mT and the frequencies used were 1, 10 and 115 Hz.

3. Results

3.1. Transmission electron microscopy

A representative zone of the iron sucrose sample is shown in Fig. 1. Two components can be distinguished: disperse electrodense particles, most likely due to the iron-containing inorganic part of the sample, with an average diameter of 5 nm and a less electrodense matrix expectedly

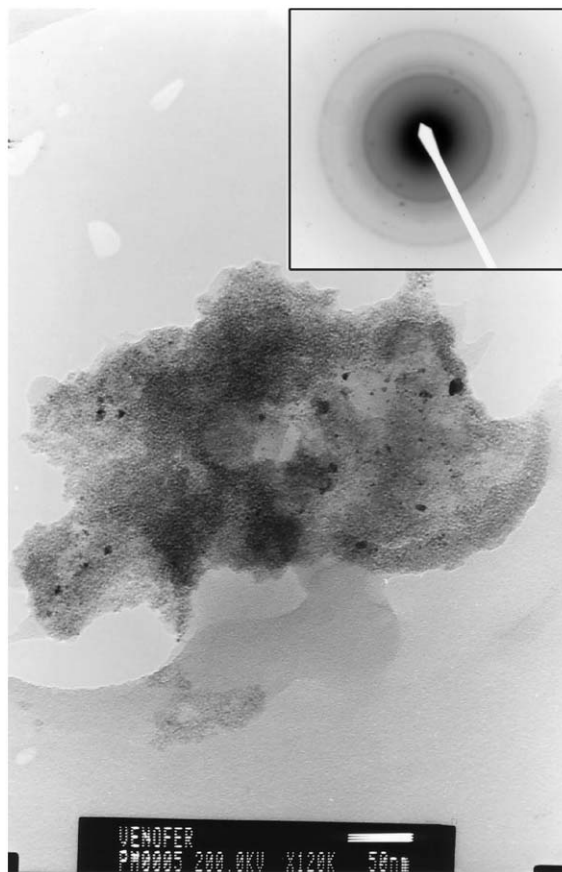


Fig. 1. Transmission electron micrograph of freeze-dried iron sucrose. The electrodense particles likely correspond to the iron oxyhydroxide. In the inset the SAED pattern of the same region is shown.

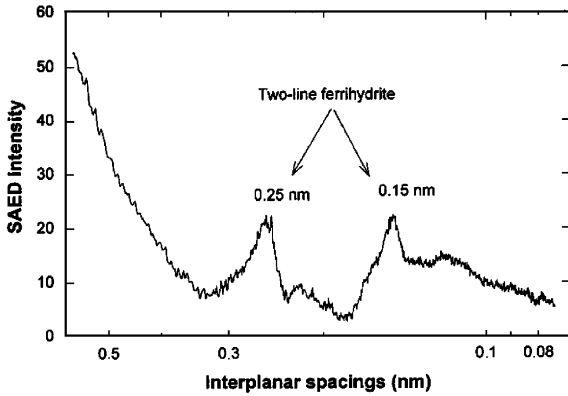


Fig. 2. Radial distribution of diffraction rings intensity corresponding to the inset in Fig. 1. The shown spectrum results after subtraction of a Gaussian background.

corresponding to the sucrose where the particles are dispersed. Selected area electron diffraction (SAED) patterns were obtained from different zones of the sample. The SAED corresponding to the image of Fig. 1 is shown as an inset. The SAED intensity profile is shown in Fig. 2. The two most intense diffraction peaks correspond to interplanar spacings of $d = 0.25$ and 0.15 nm, typical of two-line ferrihydrite [15]. Weak peaks corresponding to d values of 0.32 , 0.21 and 0.12 nm were assigned to the carbon coating the TEM grid. Additional, still identifiable, very small peaks, at 0.22 , 0.19 and 0.17 nm may correspond to incipient six-line ferrihydrite.

3.2. X-ray diffraction

The X-ray diffractogram of iron sucrose is shown in Fig. 3. The spectrum corroborates the presence of sucrose, in particular from the peaks corresponding to $d = 0.41$ and 0.67 nm [16]. Within the accuracy of the experiment, ferrihydrite peaks are seen at $d = 0.25$ and 0.15 nm corresponding to the (110) and (300) planes, respectively [17].

The average ferrihydrite crystallite size has been obtained by using the full-width at half-maximum of the (110) reflection using the Scherrer equation [18], resulting in a diameter of 5 nm (± 1 nm).

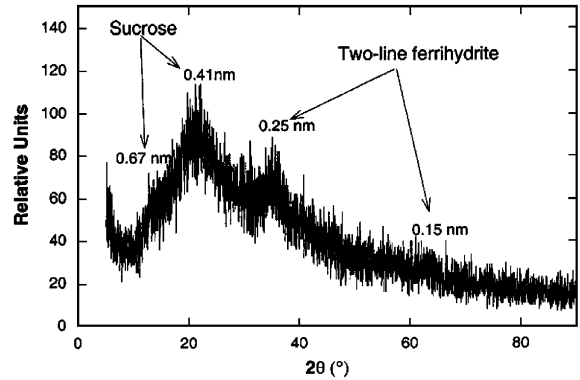


Fig. 3. X-ray diffractogram of the freeze-dried iron sucrose powder. The interplanar distances are shown in nm.

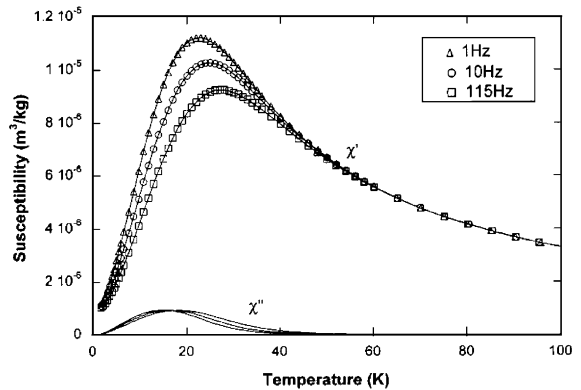


Fig. 4. Temperature dependence of the AC mass susceptibility of freeze-dried iron sucrose at three different frequencies. See the clean absence of relaxation above ≈ 50 K.

3.3. Magnetic characterisation

AC susceptibility measurements have been carried out on iron sucrose in the temperature range between 1.7 and 300 K at three different frequencies, 1 , 10 and 115 Hz. The temperature dependence of the AC susceptibility is shown in Fig. 4. The out-of-phase susceptibility χ'' is zero, within the accuracy of the experiments, above 50 K, which means that in this temperature range the in-phase susceptibility χ' coincides with the static one. χ' shows a maximum at around 25 K, for 10 Hz, accompanied by a χ'' maximum at

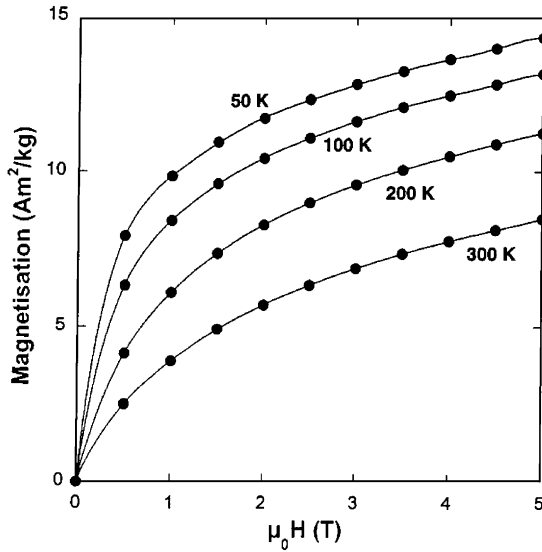


Fig. 5. Field dependence of the magnetisation of freeze-dried iron sucrose at the temperatures indicated. Zero remanence has been obtained in this temperature range. The continuous lines are just guides for the eye.

slightly lower temperatures which evidences a magnetic relaxation phenomenon.

The field-dependent magnetisation results on the same sample are shown in Fig. 5. The temperatures of the experiments have been selected in the range where the out-of-phase AC susceptibility is negligible. The data shown were taken under decreasing field, confirming the expected zero remanent magnetisation.

4. Discussion

The X-ray diffraction and the TEM/SAED results are absolutely coincident from the structural and from the particle size point of view. Therefore, the analysed iron sucrose consists of nanometric particles of about 5 nm diameter, most likely composed of two-line ferrihydrite, dispersed in a sucrose matrix.

At temperatures above 50 K, that is, where $\chi'' \approx 0$, $\chi'(T)$ coincides with the static susceptibility and can be expressed as $\chi = \chi_{SP} + \chi_{AF} + \chi_D$. In the expression, χ_{SP} is the superparamagnetic susceptibility of the particles that will follow a Curie law,

χ_{AF} the antiferromagnetic susceptibility of the iron oxyhydroxide that may slightly vary with temperature, and χ_D the total diamagnetic contribution that will be temperature independent. It is customary, in the interpretation of these type of data, to include in χ_D only the diamagnetic susceptibility of the sample holder and other addenda, however, in our case, and especially due to the low signal of the antiferromagnetic nanoparticles, the diamagnetic contribution of the excipients (e.g. sucrose) are of enough relevance to be taken into account. Since $\chi_{SP} = C/T$, it is adequate to use a χ' vs. $1/T$ representation, in order to obtain the Curie constant C . In this representation, the data ideally must form a straight line with slope C and intercept with the χ -axis equal to $\chi_{AF} + \chi_D$. In our case we have obtained a rather linear result but the slight bending observed has permitted to obtain the $(\chi_{AF} + \chi_D)$ intercept value being $-2.3 \times 10^{-7} \text{ m}^3/\text{kg}$ at 50 K and $-6.3 \times 10^{-7} \text{ m}^3/\text{kg}$ at 300 K. The negative sign of these values indicates that the diamagnetic susceptibility is indeed greater than the antiferromagnetic one. The Curie constant of any paramagnetic, but also superparamagnetic, system can be written as $C = \mu_0 N m_{\text{eff}} / (3k)$, N being the number of magnetic ions per unit volume, m_{eff} the so-called effective moment per ion and k the Boltzmann constant. By using this expression we have obtained $m_{\text{eff}} = 16.5 \pm 0.7 \mu_B$ per iron ion, where the error value responds to the slight difference in the high- and low-temperature slope determination. It has been observed experimentally that for antiferromagnetic oxide nanoparticles it is almost a general rule that the mass magnetic susceptibility increases for decreasing particle size [19]. This result indicates that the particle magnetic moment is not proportional to the particle volume, and in this respect, several models to explain the net magnetic moment per particle as result of spin uncompensation have been proposed [20]. The experimentally determined m_{eff} value, definitely higher than the single ion magnetic moment which is typically near $5 \mu_B$ for iron ions, cannot be explained with the volume uncompensation model which predicts a number of uncompensated spins in the particle proportional to square root of its number of spins, and

less by other models which restrict the spin uncompensation only to the particle surface. If any of the models is considered, the maximum expected effective moment per ion never results higher than the one corresponding to the paramagnetic ion [21]. We should, however, indicate that effective moments also of the order of 15 Bohr magnetons have previously been obtained for assemblies of two-line ferrihydrite nanoparticles in zeolitic matrices [21].

To assess the importance of dipole–dipole interparticle interactions, the temperature parameter $T_{\text{dip}} = 3C\rho/(4\pi)$ has been estimated [21]. In the expression, C is the Curie constant in mass-susceptibility representation and $\rho = 71.9 \text{ kg Fe/m}^3$ is the iron mass per unit volume in the sample. Using this calculation, T_{dip} for freeze-dried iron sucrose results in 0.13 K. This low value justifies the use of non-interaction models in the interpretation of the susceptibility results in the temperature ranges that we have studied.

The field-dependent magnetisation data corroborate what has been observed in the AC susceptibility. In this case, the magnetisation will follow the expression $M = M_{\text{SP}} + (\chi_{\text{AF}} + \chi_{\text{D}})H$, where M_{SP} is the superparamagnetic magnetisation, which will result from a collection of Langevin functions extended to the distribution of particle magnetic moments, and H is the applied field. As it usually occurs for assemblies of antiferromagnetic particles, the customary representation M vs. H/T does not result in a good superposition of the data unless the $(\chi_{\text{AF}} + \chi_{\text{D}})$ term is considered. However, it is known that χ_{AF} is typically temperature dependent [22], complicating the analysis. The best overlap in our case has been obtained by considering $(\chi_{\text{AF}} + \chi_{\text{D}})$ values of the order of the susceptibility intercepts given above.

An alternative way of estimating the importance of the interparticle interactions, and especially in what may affect the magnetic dynamics of the system, consists in the use of a scaling plot where χ'' is represented as a function of $-T \ln(\omega\tau_0)$, ω being the AC angular frequency and τ_0 a pre-exponential factor. In this representation, in the case of negligible interparticle interactions, the dynamics of the magnetic moments follows the Arrhenius model, in such a way that the χ'' vs.

$-T \ln(\omega\tau_0)$ data, taken at different frequencies, must superpose on a single master curve if a pre-exponential factor in the range of 10^{-9} – 10^{-12} s is used. In Fig. 6, the results for 1, 10 and 115 Hz are represented having optimum superposition at $\tau_0 = 10^{-14}$ s. This value is close to the expected one in a non-interacting model, as also has been the case of iron sorbitol [13], but undoubtedly not unphysical as observed in iron dextran [14].

In Fig. 7, the iron sucrose $\chi''(T)$ profile has been plotted together with previous results on iron dextran [14]. The iron sucrose $\chi''(T)$ profile is definitely narrower and it has a much simpler, bell-shaped, aspect than that of iron dextran. The $\chi''(T)$ profile represents the activation energy distribution and can be interpreted as a measure of the particle size distribution in the case of assemblies of non-interacting particles.

The TEM results, that indicate that the iron-containing particles in iron sucrose are smaller than those in iron dextran ($4 \times 20 \text{ nm}$), suggest that the iron dextran $\chi''(T)$ profile may not be too bad an estimate of its actual particle size distribution if the same effective anisotropy constant is assumed, although in that case, the dynamics did not correspond clearly to a non-interaction model, and the particle structure was interpreted as akaganéite.

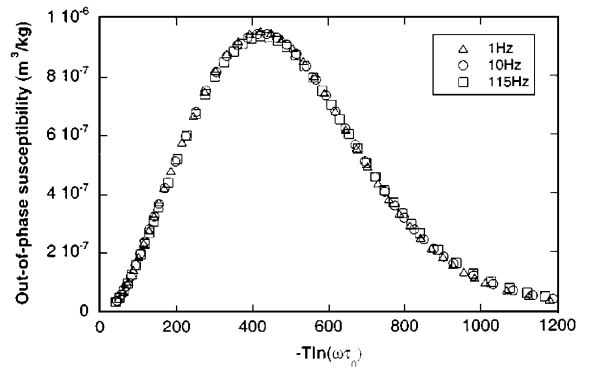


Fig. 6. Scaling plot of the out-of-phase mass susceptibility of freeze-dried iron sucrose measured at three different frequencies. The best fit is obtained with a preexponential factor of $\tau_0 = 10^{-14}$ s.

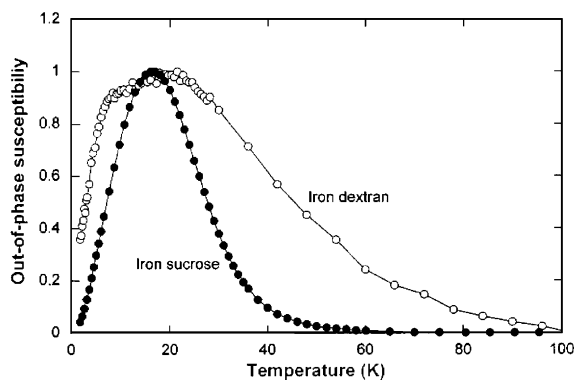


Fig. 7. Comparison of the temperature dependence of the out-of-phase susceptibility of iron sucrose (this work) and iron dextran (data from Ref. [14]).

5. Conclusions

Freeze-dried iron sucrose contains small superparamagnetic particles, of an approximated size of 5 nm, whose structure is close to two-line ferrihydrite. The particles are dispersed in a sucrose matrix and do not present evident signs of aggregation.

The $\chi''(T)$ iron sucrose profile is narrower, its shape is more simple and the magnetic dynamics better corresponds to the non-interacting model than in the case of iron dextran. This result may be advantageously used in potential magnetic monitoring of biological processes employing this drug. This same profile may also be of interest in order to compare different iron-containing drugs for it is not affected by extra diamagnetic and paramagnetic contributions. Still, the possible relaxation contribution associated with the antiferromagnetism of the particles should be an effect of much less importance.

The magnetic characterisation of iron-containing drugs has also been proven to be of much interest to study the state of iron, because of its specificity to magnetogenic ions in cases like these, where iron is present in a small amount with respect to the organic matrix. In this respect, this technique has a higher sensitivity than other conventional structural techniques.

The magnetic behaviour of two-line ferrihydrite nanoparticles has been much less explored than other iron oxides/oxyhydroxides. This study gives

a new example of the effective ferrimagnetic behaviour (uncompensated antiferromagnetism) of two-line ferrihydrite nanoparticles.

Acknowledgements

The authors thank M.S. Romero and A.R. Abadía for very fruitful discussions. Spanish MCYT, under Grant PB98-1606 is also acknowledged.

References

- [1] J.Q. Hudson, T.J. Comstock, Clin. Ther. 23 (2001) 1673.
- [2] B.G. Danielson, T. Salmonson, et al., Arzneimittel Forsch. 46 (1996) 615.
- [3] D.B. Van Wyck, G. Cavallo, et al., Am. J. Kidney Dis. 36 (2000) 88.
- [4] W.H. Hörl, Am. J. Kidney Dis. 37 (2001) 859.
- [5] C. Charytan, M.H. Schwenk, M.M. Al-Saloum, et al., Nephron Clin. Pract. 96 (2004) C63.
- [6] H.J. Manley, D.W. Grabe, BMC Nephrology 5 (2004) 1.
- [7] K. Geetha, M.S.S. Raghavan, et al., Carbohydr. Res. 271 (1995) 163.
- [8] F. Funk, G.J. Long, D. Hautot, et al., Hyperfine Interact. 136 (2001) 73.
- [9] P.R. Marshall, D. Rutherford, J. Colloid Interface Sci. 37 (1971) 390.
- [10] K.M. Towe, J. Biol. Chem. 256 (1981) 9377.
- [11] B. Knight, L.H. Bowen, R.D. Bereman, et al., J. Inorg. Biochem. 73 (1999) 227.
- [12] M.I. Oshtrakh, V.A. Semionkin, et al., Z. Naturforsch. 55a (2000) 186.
- [13] F.J. Lázaro, A. Larrea, A.R. Abadía, M.S. Romero, J. Magn. Magn. Mater. 250 (2002) 256.
- [14] F.J. Lázaro, A. Larrea, A.R. Abadía, J. Magn. Magn. Mater. 257 (2003) 346.
- [15] D.E. Janney, J.M. Cowley, P.R. Buseck, Clay Miner. 48 (2000) 111.
- [16] JCPDS-International Centre for Diffraction Data (Ref: Natl. Bur. Stand. (US) Monogr. 25 (11) (1974) 66.
- [17] R.M. Cornell, U. Schwertmann, The Iron Oxides: Structure, Properties, Reactions, Occurrence and Uses, VCH, Weinheim, 1996.
- [18] L.V. Azaroff, Elements of X-ray Crystallography, McGraw-Hill, New York, USA, 1968.
- [19] J. Cohen, K.M. Creer, et al., J. Phys. Soc. Japan 17 (Suppl. B1) (1962) 685.
- [20] L. Néel, J. Phys. Soc. Japan 17 (Suppl. B1) (1962) 676.
- [21] A. López, F.J. Lázaro, J.L. García-Palacios, et al., J. Mater. Res. 12 (1997) 1519.
- [22] S.A. Makhlof, F.T. Parker, A.E. Berkowitz, Phys. Rev. B 55 (1997) R14717.